0026-895X/05/6704-1128–1136$20.00
MOLECULAR PHARMACOLOGY
Vol. 67, No. 4
6346/1198131

Mol Pharmacol 67:1128–1136, 2005
Printed in U.S.A.

Molecular Interactions between Matrilysin and the Matrix Metalloproteinase Inhibitor Doxycycline Investigated by Deuterium Exchange Mass Spectrometry[S]

Ricardo A. García, Dennis P. Pantazatos, Christopher R. Gessner, Katrina V. Go, Virgil L. Woods, Jr., and Francisco J. Villarreal

Department of Medicine, University of California, San Diego, California

Received August 17, 2004; accepted January 21, 2005

ABSTRACT

Matrix metalloproteinases (MMPs) play an essential role in normal and pathological extracellular matrix degradation. Deuterium exchange mass spectrometry (DXMS) was used to localize the binding regions of the broad-spectrum MMP inhibitor doxycycline on the active form of matrilysin (residues 95–267) and to assess alterations in structure induced by doxycycline binding. DXMS analyses of inhibitor-bound versus inhibitor-free forms of matrilysin reveal two primary sites of reduced hydrogen/deuterium exchange (residues 145–153; residues 193–204) that flank the structural zinc binding site. Equilibrium dialysis studies of doxycycline-matrilysin binding yielded a K_d of 73 μM with a binding stoichiometry of 2.3 inhibitor molecules per protein, which compares well with DXMS results that show principal reduction in deuterium exchange at two sites. Lesser changes in deuterium exchange evident at the amino and carboxyl termini are attributed to inhibitor-induced structural fluctuations. Tryptophan fluorescence quenching experiments of matrilysin with potassium iodide suggest changes in conformation induced by doxycycline binding. In the presence of doxycycline, tryptophan quenching is reduced by approximately 17% relative to inhibitor-free matrilysin. Examination of the X-ray crystal structure of matrilysin shows that the doxycycline-binding site at residues 193 to 204 is positioned within the structural metal center of matrilysin, adjacent to the structural zinc atom and near both calcium atoms. These results suggest a mode of matrilysin inhibition by doxycycline that could involve interactions with the structural zinc atom and/or calcium atoms within the structural metal center of the protein.

Remodeling of the extracellular matrix (ECM) is critical for the maintenance of life. Important physiological processes that depend on efficient remodeling of ECM include organ growth and morphogenesis, tissue repair, embryonic development, and general maintenance of cell and tissue structural support. Tight regulation of these processes is vital for proper physiological function. Aberrant remodeling of ECM can have deleterious effects on tissue structural stability and physiological function and can lead to pathological tissue remodeling.

Degradation of ECM is catalyzed by ubiquitous enzymes called matrix metalloproteinases (MMPs). The specificity of ECM cleavage by MMPs is broad: MMPs can cleave virtually any ECM component (Egeblad and Werb, 2002). So far, more than 25 forms of MMPs have been identified in vertebrates, suggesting more global roles for MMPs in tissue remodeling (Lindsey, 2004). MMPs are members of the zinc-dependent metallopeptidases (Visse and Nagase, 2003). Members of this family typically contain an autoinhibitory pro domain, a catalytic zinc-binding domain that operates via a "cysteine switch" mechanism (Wart and Birkedal-Hansen, 1990), and a substrate-binding hemopexin-like domain (Visse and Nagase, 2003). In addition, MMPs contain a second zinc atom and at least two calcium atoms that are not part of the catalytic center and seem to play roles in stabilizing tertiary structure (Lowry et al., 1992; Willenbrock et al., 1995). MMPs are expressed as zymogens (pro-MMPs), and are either secreted from the

This work was supported by National Institutes of Health grants 2-R01-HL43617-10A2 (to F.V.) and CA099835 (to V.W.), and by University of California BioStar grants S97-90 and S99-44 and LSI program L98-30 (to V.W.). The matching corporate sponsor for these grants was ExSAR Corporation (Monmouth Junction, NJ), in which V.W. has an equity interest. Support for R.G. was provided by a training grant from the National Institutes of Health, Cardiovascular Physiology and Pharmacology Training Program UC San Diego (2-T32-HL07444-21). The laboratories of F.V. and V.W. contributed equally to this work.

[S] The online version of this article (available at http://molpharm.aspetjournals.org) contains supplemental material.

Article, publication date, and citation information can be found at http://molpharm.aspetjournals.org.
doi:10.1124/mol.104.006346.

ABBREVIATIONS: ECM, extracellular matrix; DOX, doxycycline; MMP, matrix metalloproteinase; DXMS, deuterium exchange mass spectrometry; MOPS, 3-(*N*-morpholino)propanesulfonic acid; K_{SV}, Stern-Volmer constant; K_Q, quenching constant.

cell to the extracellular space or are anchored to the cell membrane via a transmembrane domain. The accepted paradigm for in vivo activation of most pro-MMPs involves conversion of extracellular pro-enzyme to the catalytically active form via proteolytic removal of the pro domain (Visse and Nagase, 2003). Alternate in vivo activation pathways have been proposed, including direct proteolytic activation by other MMPs (Nagase, 1997), autolytic activation via sulfhydryl oxidation of the catalytic cysteine residue (Fu et al., 2001), and protease-independent pro-MMP activation via sulfhydryl modification of the catalytic cysteine residue (Okamoto et al., 2001).

Matrilysin (also called MMP-7) is the smallest member of the MMP family and lacks the hemopexin-like domain. Matrilysin has been linked to a number of pathological processes ranging from inflammatory diseases (Matsuno et al., 2003) to heart failure (Boixel et al., 2003) and colorectal, prostate, and breast cancers (Adachi et al., 1999; Davies et al., 2001; Heppner et al., 1996). Of these processes, its purported involvement in cancer is by far the most documented. Studies using a mouse model of acinar-to-ductal pancreatic metaplasia revealed that deletion of the matrilysin gene inhibited the development of cancerous pancreatic lesions after ductal ligation (Crawford et al., 2002). Likewise, in a mouse model of multiple intestinal neoplasia, matrilysin gene knockout resulted in reduction of tumor multiplicity and a significant decrease in tumor diameter (Wilson et al., 1997). Such studies have brought much attention to matrilysin as a potential therapeutic target for small-molecule inhibitor development.

Doxycycline is the only clinically-approved drug used to inhibit MMP activity and is marketed under the name of Periostat (CollaGenex) for use in the treatment of periodontitis (Peterson, 2004). Doxycycline is a member of the tetracycline family of antibiotics and is known to exert biological effects that are independent of its antimicrobial activity. Doxycycline has been used for the experimental treatment of other pathological conditions that involve MMPs, such as aortic aneurysms (Thompson and Baxter, 1999), myocardial infarction (Villarreal et al., 2003), and cancer (Onoda et al., 2004). Although the primary mechanism of action of doxycycline on attenuating ECM degradation is ascribed to its MMP-inhibitory capacities, it remains unclear how doxycycline mediates inhibition.

Given the importance of matrilysin in the pathological progression of the diseases described, we sought to characterize critical sites of inhibitor-protein interactions on matrilysin with the broad-spectrum MMP inhibitor doxycycline. We used an enhanced form of deuterium exchange mass spectrometry (DXMS) (Woods and Hamuro, 2001; Hamuro et al., 2002b, 2003; Woods, 2002) and equilibrium dialysis to localize putative drug-binding regions on the protein and to correlate them with the determined number of drug molecules bound per protein. DXMS studies were performed without *a priori* knowledge of the drug binding sites on the protein, demonstrating the utility of DXMS in identifying and characterizing drug-binding regions on proteins. The studies presented herein suggest a mechanism for doxycycline inhibition of matrilysin activity via drug interactions with the structural zinc and/or calcium atoms of the protein.

Materials and Methods

Materials. Matrilysin was obtained from Calbiochem (San Diego, CA). Doxycycline and Sigmacote were purchased from Sigma-Aldrich (St. Louis, MO) and [^{3}H]doxycycline (specific activity, 5 Ci/mmol) was from American Radiolabeled Chemicals, Inc (St. Louis, MO). Formic acid and common reagents were purchased from Fisher Scientific (Fairlawn, NJ). D_20 (99.9%) was from Isotec (Miamisburg, OH).

Equilibrium Dialysis of Matrilysin-Doxycycline Complex. Equilibrium dialysis experiments were performed under optimized conditions for preservation of enzyme stability. Attempts to perform experiments in buffer containing moderate to high doxycycline (>200 μM) with high calcium (>1 mM) concentrations resulted in protein precipitation. Samples of purified matrilysin were diluted to 1 and 10 μM in buffer containing 50 mM HEPES, 150 mM NaCl, and 50 μM $CaCl_2$, pH 7.4. Volumes of 100 μl were placed into Slide-A-Lyzer Mini Dialysis units (7-kDa cutoff; Pierce Biotechnology, Rockford, IL) and dialyzed against 1050 μl of buffer in siliconized microcentrifuge tubes with 0, 0.1, 1, 10, 50, 100, 200, 500, 1000, and 1200 μM doxycycline for 20 to 24 h at room temperature. Samples with drug contained 1 μCi of [^{3}H]doxycycline. Minimum time to reach equilibrium (~10 h) was determined with nonradioactive doxycycline by absorbance at 345 nm. Sample volumes were measured at the end of each experiment. Radioactivity of entire protein sample volumes and equivalent volumes of dialysate were determined by tritium counting in 5 ml of scintillation liquid on a 1900CA Tri-Carb Scintillation Analyzer (PerkinElmer Life and Analytical Sciences, Boston, MA). Total ligand concentration in the protein compartment ($[Dox]_{protein}$) was determined from total tritium counts in the chamber (counts per minute per milliliter) and the specific activity of the radiolabeled ligand. Free ligand concentration ($[Dox]_{dialysate}$), which is the same in both compartments, was determined from tritium counts measured in the dialysate sample (counts per minute per milliliter). Concentration of doxycycline bound to matrilysin ($[DOX]_{bound}$) was the difference between total and free ligand concentration (i.e., $[DOX]_{bound} = [Dox]_{protein} - [Dox]_{dialysate}$. Data were plotted as fraction of protein containing bound drug, $[DOX]_{bound}$/[matrilysin], versus log total drug concentration, $[DOX]_{total}$. Data were analyzed by nonlinear least-squares regression with Prism (version 3.0; GraphPad Software, San Diego, CA) to determine equilibrium dissociation constant (K_d) and binding stoichiometry. Values are reported as mean ± S.D.

IC_{50} Determination. Inhibition of matrilysin activity by doxycycline was measured by absorbance spectroscopy using a colorimetric peptide substrate and with purified collagen in a gel-based assay. Colorimetric assays were performed with MMP-thiopeptolide substrate (BIOMOL Research Laboratories, Plymouth Meeting, MA). Assays contained 0.6 μM matrilysin in buffer [50 mM HEPES, 150 mM NaCl, 50 μM $CaCl_2$, and 1 mM 5,5′-dithiobis(2-nitrobenzoic acid), pH 7.4] in the presence of increasing concentrations of doxycycline (0, 0.1, 1, 5, 10, 50, 100, 500, and 1000 μM). Protein was incubated with drug for 1 h at 37°C in the dark. Cleavage reactions were started by addition of substrate to a final concentration of 100 μM MMP-thiopeptolide substrate. Kinetic readings were measured at 430 nm every 90 s for 1 h. Substrate cleavage rates were determined from the linear regions of kinetic curves. IC_{50} was determined from graphs of MMP activity versus log [doxycycline].

Gel-based inhibition assays were conducted with type I collagen purified from newborn rat skin as described previously (Miller and Rhodes, 1982). Purified collagen was dispersed in 0.5 M acetic acid and extensively dialyzed against buffer (50 mM HEPES and 150 mM NaCl, pH 7.4) using Slide-A-Lyzer cassettes (10 kDa cutoff; Pierce Biotechnology). Amount of collagen used for cleavage assays was determined empirically by visualization of undigested collagen band intensity in Coomassie-stained SDS-polyacrylamide gels: a single concentration that yielded intense resolvable bands was used. Matrilysin (5 μM) was incubated in buffer (50 mM HEPES, 150 mM

NaCl, and 45 μM $CaCl_2$ pH 7.4) in the absence and presence of doxycycline (0.1, 1, 10, 100, 500, 1000, and 5000 μM) at room temperature for 30 min. Collagen was added (~50 μg) to tubes, incubated at 37°C for 1 h, and run on SDS-polyacrylamide gels. Collagen band intensities were quantified by densitometry using Image J (1.31v) and IC_{50} was estimated from graphs.

Deuterium Labeling Experiments. Samples of matrilysin (80 μM in 10 mM HEPES, pH 7.4, 100 mM NaCl, and 250 μM $CaCl_2$) were complexed with the MMP inhibitor doxycycline (8.3 mM) for 30 min at room temperature and chilled on ice for 5 min. Proteins were deuterated by diluting samples into deuterium exchange buffer (20 mM MOPS, pH 7.4, 50 mM NaCl, and 1 mM dithiothreitol; 70% D_20) for a final doxycycline concentration of 2.5 mM. Samples were immediately incubated on ice for indicated times (10, 100, 1000, and 10,000 s), deuterium exchange was stopped by addition of quench buffer (30 μl of 0.8% formic acid, 0.8 M guanidine-HCl), quickly frozen in dry ice, and stored at −80°C for subsequent analyses by mass spectrometry. Nondeuterated control experiments were processed as above in nondeuterated buffer.

Mass Spectrometry Experiments. Protein samples were processed as described previously (Hamuro et al., 2003). In brief, denatured deuterated samples were fragmented with a pepsin 20-AL column [porcine pepsin (Sigma) coupled to 20AL support material (Applied Biosystems, Foster City, CA)]. Fragmented samples were passed through a coupled C18 column for reverse-phase separation of peptides (1 mm × 50 mm; Grace Vydac, Columbia, MD) using a linear acetonitrile gradient of 5% to 45% over 10 min at a flow rate of 50 μl per minute. For precise temperature control, valves, tubing, columns, and auto-sampler were refrigerated at 2.8°C with columns immersed in a melting ice bath. Effluent from the C18 column was analyzed on both a Thermo Finnigan LCQ electrospray mass spectrometer (Thermo Electron Corporation, Woburn, MA) and a Micromass quadrupole time-of-flight mass spectrometer (Waters, Milford, MA). Data were collected for each run and saved for subsequent data analyses.

DXMS Data Analysis. DXMS analysis was used to confirm sequence identity and track time-dependent deuterium buildup for all proteolyzed peptides. In brief, the SEQUEST program (Thermo Electron Corporation) was used to identify the likely amino acid sequence of peptide fragments and analyzed as described previously (Woods, 2002; Pantazatos et al., 2004). DXMS analysis was performed using SEQUEST output MS1 and MS2 data (i.e., the parent and daughter tandem mass spectrometric data). SEQUEST identifications were confirmed with DXMS by comparing the predicted isotopic envelopes for the proteolyzed peptides generated from SEQUEST against MS1 data acquired from the Q-TOF mass spectrometer. DXMS data reduction was used to track deuterium buildup for each peptide fragment over time (10, 100, 1000, and 10,000 s). Selected peptides passing this automated quality-control step were manually checked for correct fit and mass identification (Pantazatos et al., 2004). Peptide maps were generated from DXMS data showing localized areas of deuterium buildup on each peptide fragment over time. Areas in which deuterium exchange was localized were colored red, and areas without deuterium were colored blue. Specific locations of deuterium within matrilysin were assigned by forming a consensus map of deuterium exchange within regions of overlapping peptides, as described previously (Pantazatos et al., 2004).

Fluorescence Quenching of Matrilysin. Fluorescence measurements were performed using an AlphaScan fluorometer (Photon Technology International, Lawrenceville, NJ) at room temperature with an excitation wavelength of 285 nm and slit widths of 8 nm. Tryptophan emission spectra for each sample were measured from 300 to 400 nm. Spectra were taken in 1-nm increments with 1 s of integration per increment. Protein samples of 5 μM were prepared in buffer (50 mM HEPES, 100 mM KCl, and 50 μM $CaCl_2$, pH 7.4) with either 0 or 400 μM doxycycline and incubated in the dark for 30 min at room temperature. Competitive absorbance by doxycycline precluded use of higher drug concentrations. Titrations were conducted with freshly prepared potassium iodide (5 M stock solution) supplemented with 0.1 mM sodium thiosulfate to prevent oxidation of iodide. Quenching of tryptophan emission was performed by successive additions of potassium iodide (50–500 mM) to the cuvette. The sample was gently mixed, incubated for 3 min after each addition of potassium iodide, and the spectra were recorded.

Analysis of Fluorescence Quenching Data. Iodide quenching data were analyzed according to the Stern-Volmer and modified Stern-Volmer equations (Lakowicz, 1983). Under conditions in which static and collisional quenching do not occur simultaneously, the Stern-Volmer relationship is represented by $F_0/F = 1 + K_{SV}$ [Q] (1).

where K_{SV} is the collisional Stern-Volmer quenching constant, F_0 and F are the fluorescence intensities in the absence and presence of quencher, respectively, and [Q] is the quencher concentration. A plot of F_0/F as a function of [Q] yields a linear plot for homogeneous fluorescence emitters, all equally accessible to quencher, whose slope is equal to K_{SV}. A heterogeneous population of fluorophores indicates that only a fraction of fluorophores is accessible to quencher and results in downward curvature of the Stern-Volmer plot (Lakowicz, 1983). For such cases, the modified Stern-Volmer equation is used: $F_0/(F_0 - F) = 1/\{[Q]\ f_a\ K_Q\} + 1/\ f_a$, where f_a is the fraction of the fluorescence accessible to quencher and K_Q is the quenching constant. A plot of $F_0/(F_0 - F)$ as a function of 1/[Q] yields a linear plot with a slope equal to $1/f_aK_Q$ and a y-intercept of $1/f_a$.

Results

Doxycycline-Matrilysin Dissociation Constant and Binding Stoichiometry. The dissociation constant (K_d) and binding stoichiometry of the doxycycline-active matrilysin (residues 95–267; hereafter referred to as "matrilysin") complex was determined by equilibrium dialysis. Minimum time required for doxycycline to equilibrate between buffer and protein compartments was 10 h: subsequent experiments with protein were performed for 24 h. A representative binding experiment is shown in Fig. 1. The binding isotherm shows that matrilysin achieves saturation with doxycycline at millimolar concentrations of drug. Data plotted as saturation fraction versus free doxycycline concentration were analyzed by nonlinear least-squares fitting and revealed a K_d of 73 ± 8 μM and a binding stoichiometry of 2.3 ± 0.2. To control for Donnan effects, parallel equilibrium dialysis ex-

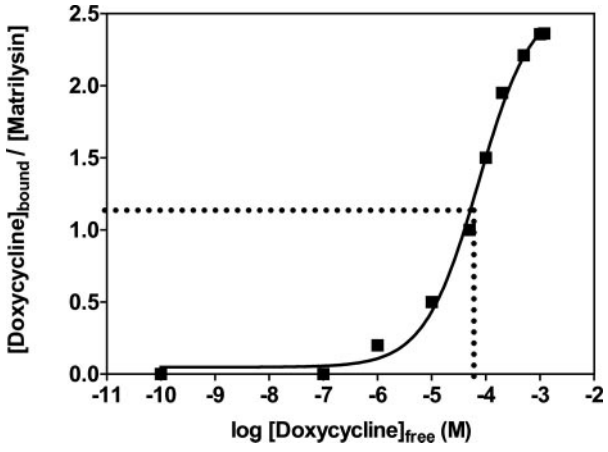

Fig. 1. Determination of dissociation constant (K_d) and binding stoichiometry for doxycycline-matrilysin complex by equilibrium dialysis. Representative graph of equilibrium binding of matrilysin-doxycycline complex is shown. Analyses of binding data by nonlinear least-squares revealed a K_d of 73 ± 8 μM and a binding stoichiometry of approximately 2.3 doxycycline molecules bound per protein monomer. Experiments were performed at least in triplicate.

periments were carried out at higher ionic strengths (Suter and Rosenbusch, 1977) and showed no effects on equilibrium (data not shown).

Inhibition of Matrilysin Activity by Doxycycline. To address conflicting data in the literature regarding the capacity of doxycycline to inhibit matrilysin (Kivela-Rajamaki et al., 2003; Peterson, 2004), doxycycline-mediated inhibition of matrilysin was demonstrated with a commonly used matrix metalloproteinase-specific peptide substrate (colorimetric substrate) and with native type I collagen. Cleavage of colorimetric peptide substrate in the presence of increasing concentrations of doxycycline yielded an IC_{50} value of 28 ± 5 μM. Detailed analyses of IC_{50} data for this substrate are provided (see Supplemental Materials). Additional experiments to assess inhibition by doxycycline with a more physiologically relevant substrate were conducted with native collagen purified from rat. In these experiments, the degree of preservation of collagen is indicative of doxycycline inhibition. The gel in Fig. 2A shows two bands at molecular masses of approximately 138 and 128 kDa that correspond to uncleaved α-chains of collagen. Complete in vitro cleavage of collagen occurs in the presence of matrilysin (5 μM) and decreases in the presence of increasing doxycycline (Fig. 2A). Densitometric analyses of collagen band intensities revealed an IC_{50} of 90 ± 31 μM for inhibition of collagen degradation (Fig. 2B).

DXMS Studies of Doxycycline-Matrilysin Complex. DXMS was used to map the binding regions of doxycycline on matrilysin and to assess local changes in tertiary structure induced by drug binding. Deuterium on-exchange was performed in deuterated buffer under conditions that favored >97% doxycycline-matrilysin complex formation based on the calculated K_d reported above. Figure 3A shows fragmentation maps for matrilysin and matrilysin-doxycycline complex taken at the earliest deuterium on-exchange time point (10 s). Protein fragmentation and subsequent filtering of fragments for quality (described by Hamuro et al., 2003) resulted in 114 overlapping peptide fragments that covered the entire length of the protein. Discrete changes in deuterium exchange are evident at various locations of the protein. The most prominent changes in deuterium exchange that occur after drug binding are evident at two sites (residues 145–153 and residues 193–204; magenta circles) that flank the structural zinc-binding region (from primary amino acid sequence). In the absence of drug, extensive deuterium exchange occurs within the consensus regions depicted in the fragmentation map (magenta circles, upper map). Upon drug binding, the degree of deuterium exchange decreases dramatically at these two sites (magenta circles, bottom). These results are in good agreement with the determined binding stoichiometry of approximately 2.3 doxycycline molecules per matrilysin monomer, indicating that these sites may represent sites of drug binding. Lesser changes in deuterium exchange are also apparent at the amino and carboxyl termini, the former being largely composed of an unstructured loop region (Browner et al., 1995). By contrast, no major changes in deuterium exchange are evident at the catalytic zinc region (residues 210–230; green circle) or the structural zinc region (residues 156–175; blue circle), indicating that drug binding does not affect deuterium exchange at these sites. Graphical representation of deuterium incorporation throughout the length of protein is shown in Fig. 3B. As expected, longer durations of deuterium on-exchange (100–10,000 s) give rise to increased deuterium incorporation throughout the protein, including locations that were shown to be exchange resistant at 10 s, most notably the zinc binding sites (Fig. 4, A–C).

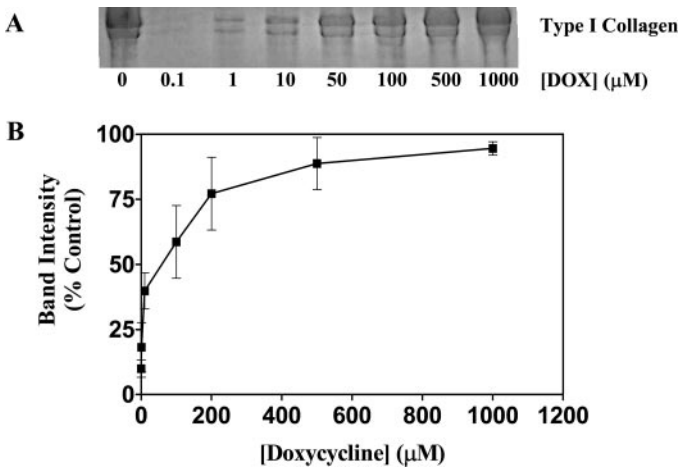

Fig. 2. Doxycycline inhibits degradation of native collagen by matrilysin. Type I collagen purified from rat was subjected to proteolysis by matrilysin. A, collagen degradation by matrilysin was analyzed by SDS-PAGE. The gel shows preservation of collagen bands as a function of increasing doxycycline concentration. Undigested control (C) is shown at left. B, the corresponding graph shows values for collagen band intensities as a percent of undigested control with respect to doxycycline concentration. Estimated IC_{50} for inhibition of collagen degradation was 90 μM.

Locations of key peptides showing enhanced or diminished deuterium exchange caused by doxycycline binding were mapped onto the three-dimensional structure of human matrilysin (Browner et al., 1995). Figure 5A shows regions of deuterium-exchange flux at the amino (residues 95–110) and carboxyl (residues 250–257) termini in the presence and absence of doxycycline and the corresponding rates of deuterium exchange. The amino-terminal region, which is largely unstructured, reveals diminished deuterium-exchange after drug binding (Fig. 5A, top graph). By contrast, residues 250 to 257, comprising a short α-helix [helix C (Browner et al., 1995)] at the carboxyl terminus, show increased deuterium exchange when bound to doxycycline (Fig. 5A, bottom graph), which is indicative of alterations in structure or dynamics (Hamuro et al., 2002a, 2003; Pantazatos et al., 2004). Residues 156 to 177 comprise a large part of the structural metal center for matrilysin, where several important metal-coordination ligands for the structural zinc and calcium atoms are located (Browner et al., 1995). Approximately 73% of this amino acid stretch is unstructured loop. The patterns of deuterium exchange observed for the loop region are similar for inhibitor-free or inhibitor-bound matrilysin, albeit slightly less in the presence of drug (Fig. 5B, top graph), indicating that this region is generally unaffected by doxycycline binding. Residues 210 to 230 contain three critical histidine residues that coordinate with the catalytic zinc (His218, His222, and His228). Doxycycline binding does not show major effects on deuterium exchange from 10 to 100 s, relative to unbound matrilysin. However, increased deuterium exchange is evident at later time points (1000 and 10,000 s; Fig. 4B, bottom graph). Residues 145 to 153 and 193 to 204 are positioned within regions that show extensive reductions in deuterium exchange based on fragmentation

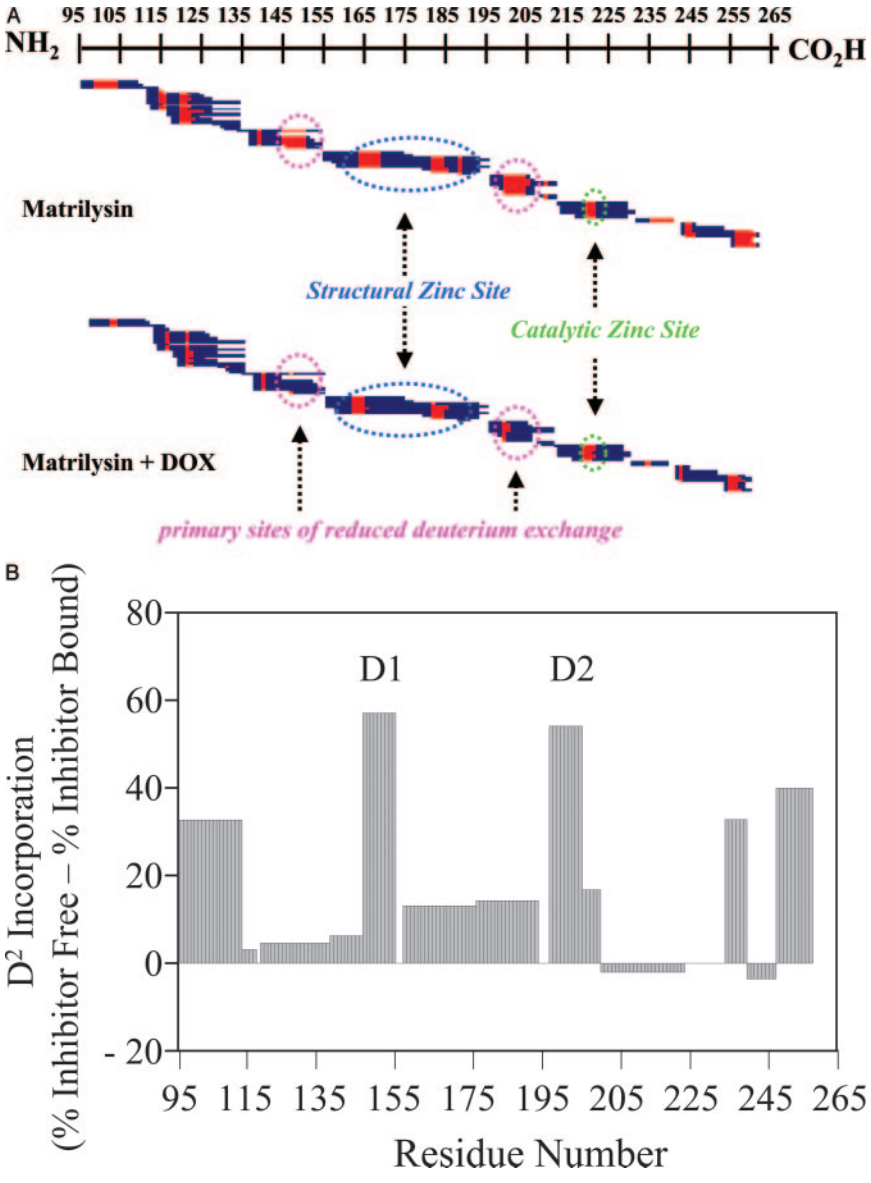

Fig. 3. Amide hydrogen/deuterium exchange maps for matrilysin. Top fragmentation map represents inhibitor-free matrilysin, and bottom map represents doxycycline-matrilysin complex. Horizontal blue bars represent fragmented matrilysin peptides generated by proteolysis. Individual peptides were color-coded red to reflect the number of deuterons that were incorporated onto each peptide. Deuterium incorporation sites were determined by optimizing consensus regions of deuterium content based on patterns of deuterium exchange of overlapping fragments. Deuterons outside of consensus regions were clustered together in the center of unresolved peptide fragments (Pantazatos et al., 2004). As denoted by the magenta circles, primary sites of reduced deuterium exchange are readily detected at sites flanking the structural zinc-binding region (blue circle). Green circle represents the catalytic zinc site. Additional regions showing lesser reductions in deuterium exchange are evident at the amino and carboxyl termini. Sequence number of residues is shown at top. B, bar graph showing percent difference in deuterium incorporation between inhibitor-free and inhibitor-bound matrilysin at fastest exchange time point (10 s) with single representative peptides spanning length of protein. Positive values reflect reduced deuterium incorporation, and negative values reflect increased incorporation relative to inhibitor-free matrilysin. Two regions implicated in doxycycline binding (D1 and D2) show the greatest reduction in deuterium exchange. Residue numbers for matrilysin are given in the *x*-axis.

maps (Fig. 3A). Residues 145 to 153 are located within β-strand 2 (Browner et al., 1995) distal to the metal binding face of the protein (Fig. 5C), whereas residues 193 to 204 make up β-strand 5, near the structural zinc and calcium atoms (Fig. 5C). In the presence of doxycycline, these residues show large decreases in deuterium exchange at 10 s (~60% and 40%, respectively; Fig. 5C). Residues 193 to 204 exhibit resistance to deuterium exchange in the drug-bound state, which persists to the last time point at 10,000 s.

Tryptophan Fluorescence Quenching of Doxycycline-Matrilysin Complex. To explore changes in matrilysin structure induced by doxycycline binding, steady-state tryptophan fluorescence quenching experiments were performed using potassium iodide (KI). In these experiments, changes in tryptophan quenching reflect alterations in solvent accessibility of tryptophan to quencher, which implicate changes in protein conformation (Lakowicz, 1983). Changes in fluorescence intensity were monitored upon titration of matrilysin with KI. Tryptophan emission spectra obtained for inhibitor-free and inhibitor-bound matrilysin are shown in Fig. 6. From the fluorescence profiles, it is evident that the

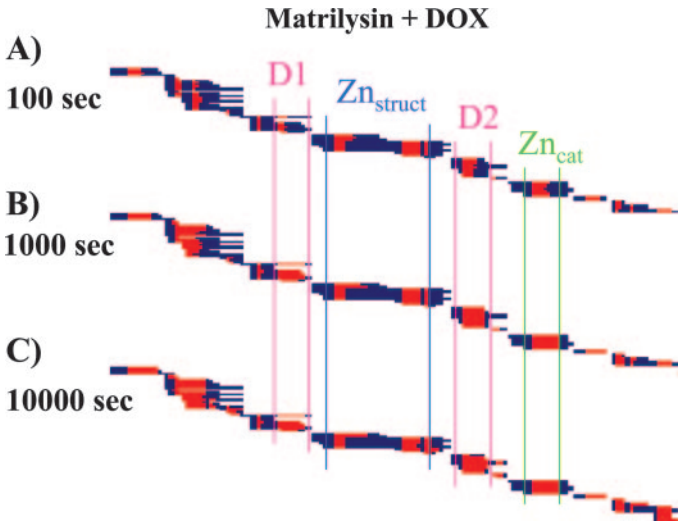

Fig. 4. Time-dependent deuterium incorporation of matrilysin-doxycycline complex. Progression of deuterium incorporation at 100, 1000, and 10,000 s. Regions of zinc binding (Zn_{struct}, blue; Zn_{cat}, green) and regions implicated in doxycycline binding (D1, D2, magenta) are shown.

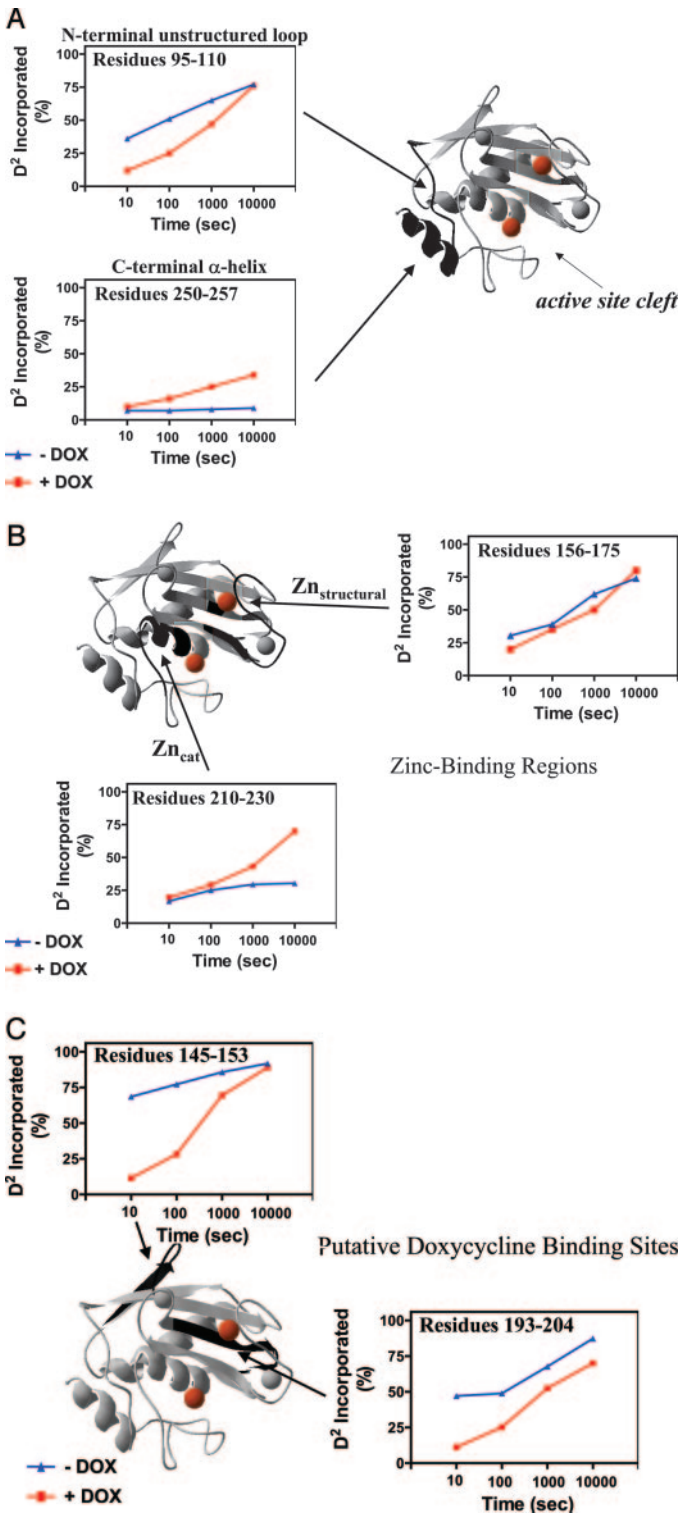

Fig. 5. Deuterium accumulation graphs and correlation to structure. Representative percentage of deuterium incorporation curves are shown for peptides from 10 to 10,000 s on-exchange. Rate of amide deuterium incorporation is dependent upon solvent accessibility and local environment of the amide. Thus, slower accumulation graphs represent regions of protection or increased stability. A, deuterium incorporation for peptides at the amino (residues 95–110) and carboxyl (250–257) termini (colored black) are shown in relation to the three-dimensional structure. B, zinc-binding regions (residues 156–175, Zn_{struct}; residues 210–230, Zn_{cat}) and (C) putative doxycycline-binding regions (residues 145–153; residues 193–204) are shown and corresponding regions on the structure are indicated (colored black). Deuterium incorporation for inhibitor-free matrilysin is colored blue (triangles), and inhibitor-bound matrilysin is colored red (squares). Three-dimensional coordinates for matrilysin (1MMQ) were downloaded from the Protein Data Bank and displayed using Swiss-PDBViewer 3.7 (http://www.expasy.org/spdbv/). Ribbon models show residues from 95 to 259. Zinc atoms are represented as orange spheres and calcium atoms are gray spheres.

peak wavelength at 325 nm for matrilysin and matrilysin-doxycycline complex does not shift to higher or lower wavelengths during the course of KI titration, indicating that KI does not disturb tertiary structure. The Stern-Volmer plots for KI quenching are shown in Fig. 6C. In the absence of doxycycline, KI quenching of tryptophan fluorescence shows a linear trend with a Stern-Volmer constant (K_{SV}) equal to 6.5 M^{-1}, which reflects homogeneity in solvent accessibility of the tryptophan residues. By contrast, exposure of matrilysin to doxycycline results in a curved plot with a downward trend indicating differential accessibility of quencher to tryptophan residues. To conduct quantitative comparisons of apo and doxycycline-bound matrilysin, modified Stern-Volmer analyses of fluorescence data were performed. The modified Stern-Volmer plots of apo and doxycycline-bound matrilysin both display linear trends, as shown in Fig. 6D. y Intercepts of 1.0 and 1.2 were determined for apo and doxycycline-bound matrilysin, respectively. The reciprocal of the y intercept represents the fraction of tryptophan fluorescence accessible to quencher (f_a) (Lakowicz, 1983). In the case of doxycycline-bound matrilysin, the f_a is 0.83, indicating that only 83% of the initial fluorescence is accessible for quenching. In addition, the quenching constant (K_Q) calculated for doxycycline-bound matrilysin 5.6 M^{-1} is smaller than apo 7.3 M^{-1}, indicating that doxycycline decreases the rate of tryptophan quenching by iodide. To ensure that iodide quenching of fluorescence was not caused by alterations in ionic strength of the solution, identical titrations were also performed using NaCl. No major decreases in fluorescence intensity caused by quenching by NaCl were observed (Fig. 5C).

Discussion

The data reported here demonstrate that doxycycline binding to matrilysin induces marked changes in deuterium exchange and tryptophan fluorescence quenching. Primary reduction in deuterium exchange occurs at residues 145 to 153 and residues 193 to 204. The latter amino acid region is adjacent to the structural zinc atom and two calcium atoms (i.e., the structural metal center of matrilysin). Quenching of tryptophan fluorescence decreases in the presence of doxycycline, suggesting that matrilysin undergoes conformational changes triggered by drug binding that decrease tryptophan accessibility to quencher. The propensity of doxycycline to bind adjacent to the structural zinc and calcium atoms is of particular interest given the ability of tetracycline to chelate calcium and zinc cations (Schneider, 2001).

Doxycycline-Binding Regions. At concentrations favoring inhibitor-protein complex formation (>97%), DXMS analyses of the doxycycline-matrilysin complex reveal two prominent regions of reduced deuterium exchange. These sites are considered protected by doxycycline binding within these regions. This assertion is drawn from several pieces of information: 1) Fragmentation mapping of matrilysin in the presence of drug shows consensus in reduced deuterium exchange for overlapping peptides at residues 145 to 153 and residues 193 to 204 (Fig. 3A). 2) Deuterium exchange rates for peptides at these locations show high degrees of protection (Fig.

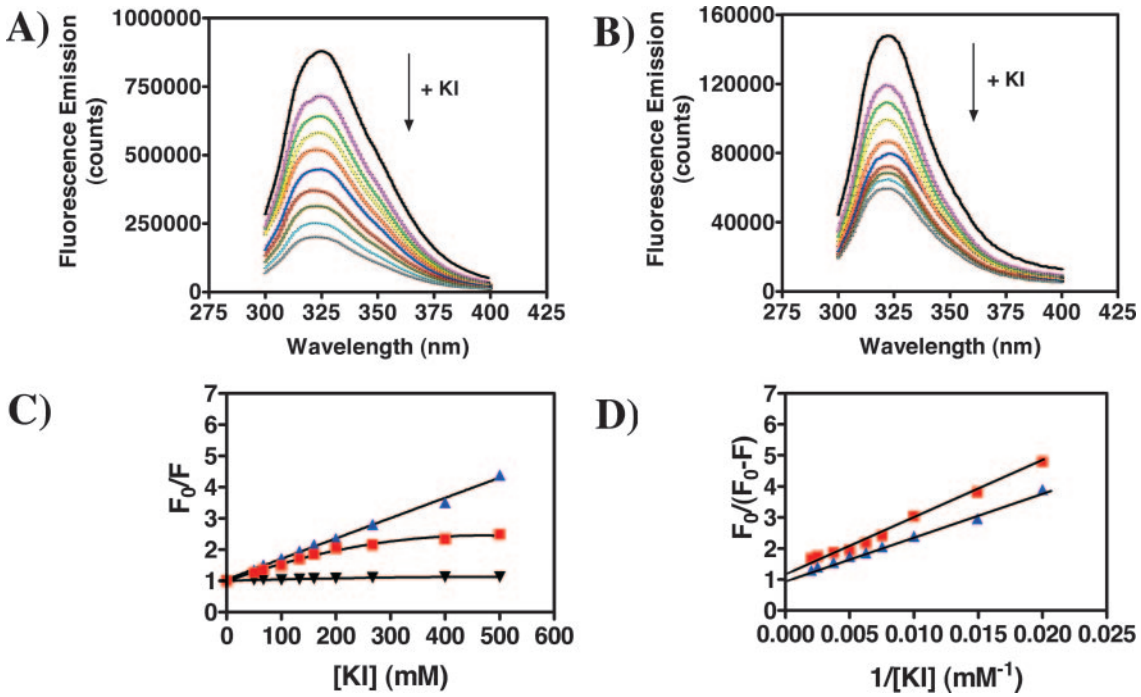

Fig. 6. Probing conformation changes in matrilysin induced by doxycycline. Potassium iodide fluorescence quenching of matrilysin in the absence (A) and presence (B) of 400 μM doxycycline. Competitive absorbance of doxycycline precluded use of higher inhibitor concentrations. C, Stern-Volmer plot with matrilysin and DOX-bound matrilysin. For inhibitor-free matrilysin (blue triangles), the plot of F_o/F as a function of [quencher] yields a linear plot indicating that all tryptophan residues are equally accessible to quencher. In the presence of DOX (red squares), the curve shows a downward trend indicating differential accessibility of tryptophan residues to quencher. Changes in tryptophan fluorescence were not caused by increases in electrolyte concentration, as indicated by NaCl titrations (black triangles). D, modified Stern-Volmer analyses indicate that tryptophan exposure of matrilysin decreases by approximately 17% in the presence of doxycycline.

5C). At 10 s, exchange at residues 145 to 153 shows a marked decrease (60%) upon doxycycline binding. Likewise, residues 193 to 204 also show high degrees of protection (40%). In addition, protection is conserved at residues 193 to 204 throughout the course of deuterium exchange, suggesting that drug binding may be more stable here than at the former location. 3) Reduced deuterium exchange at two distinct sites is in good agreement with the determined binding stoichiometry of approximately 2.3 doxycycline molecules bound per protein. Although our interpretation of these data are not unambiguous, results described here support the assertion that doxycycline binds at these two sites.

Comparisons of the amino acid content between these regions show only 16.7% sequence homology, thus ruling out a conserved sequence motif for doxycycline binding. It is interesting, however, that both amino acid regions contain a single tryptophan residue (Trp149, Trp198). This finding is significant given that tetracyclines are known to bind proteins via combined hydrophobic and electrostatic interactions (Kisker et al., 1995; Khan et al., 2002). Fluorescence studies on the tetracycline-Tet repressor protein complex showed that tetracycline binding is potentiated in the presence of divalent cations (Takahashi et al., 1986). Moreover, tetracycline was shown to be in direct proximity of a tryptophan residue in the drug-protein complex (Takahashi et al., 1986). These data imply that tryptophan residues, alone or in conjunction with protein-bound divalent metals, may represent viable sites for doxycycline (and tetracycline) interactions and/or docking. Although the studies described herein were performed in the presence of micromolar calcium, which is in agreement with concentrations known to stabilize fibroblast collagenase (Lowry et al., 1992), we cannot rule out the possibility that higher, physiological calcium levels that are present within the extracellular matrix might facilitate further binding to matrilysin.

Amino-Terminal Peptide Docking Site. Changes in deuterium exchange were also evident at the amino and carboxyl termini (Fig. 5A). The carboxyl-terminal helix forms a well defined binding site for the amino terminal peptide that is located outside of—and adjacent to—the catalytic domain. The carboxyl-terminal helix maintains several interregion contacts with the amino-terminal peptide and is proposed to function as a docking site for the amino-terminal peptide for zymogen activation (Browner et al., 1995). It is interesting that increases in deuterium exchange occur at the carboxyl terminus (residues 250 to 257) upon drug binding to matrilysin, indicating that solvent accessibility of this region has increased. These data suggest changes in protein conformation (Hamuro et al., 2002a, 2003; Pantazatos et al., 2004). By comparison, reduced deuterium exchange of the unstructured amino-terminal loop was observed at 10 s (20% decrease; Fig. 5A). The observed reduction in deuterium exchange is of lesser magnitude than that observed at residues 145 to 153 or 193 to 204 and is probably caused by stabilization of the loop region with vicinal regions of the protein, or possibly by low-affinity interactions with doxycycline present in solution. Stabilization of unstructured loop regions of proteins by ligand binding has been observed by hydrogen/deuterium exchange in several ligand-protein complexes (Hamuro et al., 2002a, 2003; Yamamoto et al., 2004).

Doxycycline-Induced Conformation Changes. Data obtained by fluorescence quenching of doxycycline-matrilysin

complex suggest changes in structure induced by drug binding. Active matrilysin contains four tryptophan residues (Trp104, Trp136, Trp149, and Trp198), three of which fall within amino acid regions that showed reductions in deuterium exchange when doxycycline was present. Quenching studies demonstrated that drug binding decreases solvent exposure of tryptophan residues (modified Stern-Volmer analyses; Fig. 6D), implying that local structure vicinal to tryptophan is altered, yielding reduced access to quencher. Trp 104 is present within the amino-terminal loop of matrilysin: the loop region is implicated in conformational rearrangement upon drug binding (discussed above). Remaining tryptophan residues may also become less accessible for quenching via local structure changes. Although our quenching studies infer changes in structure adjacent to tryptophan residues in matrilysin, the exact nature of this conformational change is as yet undetermined.

Mode of MMP Inhibition by Doxycycline. The current paradigm for inhibition of MMPs involves chelation of the catalytic zinc atom from the enzyme active site (Peterson, 2004). Structures of matrilysin reported by Browner et al. (1995) were determined in complex with three unique inhibitors containing hydroxamate, sulfodiimide, or carboxylate as the zinc-coordination group. The polar atoms of all inhibitors interact with the same main-chain atoms at the catalytic active site of matrilysin. In addition, all inhibitors were shown to form unique bonding groups with the catalytic zinc atom. Hydroxamate exhibited ideal bidentate bonding with the catalytic zinc atom for stable divalent metal coordination within the active site. By contrast, our observation that doxycycline binds proximal to the structural zinc site suggests that inhibition of the MMP matrilysin may occur without direct interactions with the catalytic zinc atom but rather via interactions with the structural zinc and/or calcium atoms contained within the structural metal center of the protein. Our results are consistent with enzyme kinetics studies with MMP-8 and MMP-13 (Smith et al., 1999) and partial-proteolysis experiments of MMP-8 (Smith et al., 1996) that support a mechanism for doxycycline inhibition of MMP activity via chelation of calcium. Chelation of the structural zinc atom by tetracyclines has also been hypothesized to inactivate MMPs via destabilization of tertiary structure (Ryan et al., 1996; Seftor et al., 1998). In this scenario, chelation of the structural zinc and/or critical calcium atoms could result in destabilization of native matrilysin structure and lead to protein denaturation and degradation. Figure 7 summarizes a proposed mode of matrilysin inhibition by doxycycline that involves chelation of either zinc or calcium from the structural metal center of matrilysin.

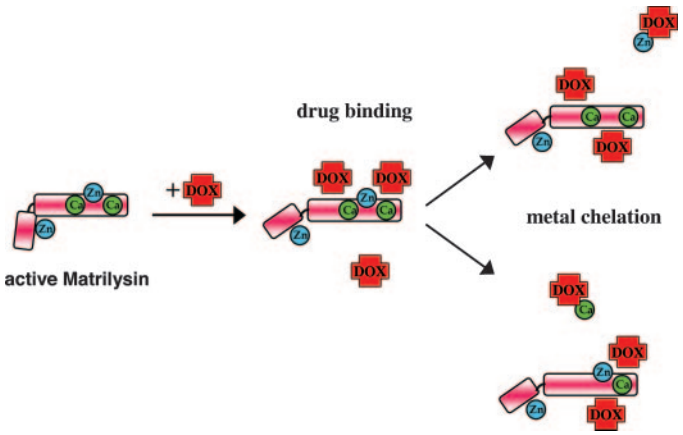

Fig. 7. Schematic depiction of matrilysin inhibition by doxycycline. Inhibition of matrilysin activity is proposed to occur via doxycycline binding proximal to the structural metal center and chelation of the structural zinc and/or calcium cations. Loss of these critical metals may lead to instability of tertiary structure.

The observed avidity of doxycycline for the structural metal center may play a key role in inhibiting matrilysin activity. Future biophysical studies to localize regions of doxycycline interactions with other classes of MMPs will aid in defining the exact mechanisms by which doxycycline inhibits MMP activity.

Acknowledgments

We are grateful to Professor Robert MacDonald (Northwestern University) for use of the fluorometer, Krissi Hewitt for assistance with early DXMS data analysis, and Neil Tolentino for help with binary maps. We also thank Prof. Joseph Adams, Prof. Seth Cohen, and Shirley Reynolds for critical reading of the manuscript.

References

Adachi Y, Yamamoto H, Itoh F, Hinoda Y, Okada Y, and Imai K (1999) Contribution of matrilysin (MMP-7) to the metastatic pathway of human colorectal cancers. *Gut* **42:**252–258.

Boixel C, Fontaine V, Rucker-Martin C, Milliez P, Louedec L, Michel JB, Jacob MP, and Hatem SN (2003) Fibrosis of the left atria during progression of heart failure is associated with increased matrix metalloproteinases in the rat. *J Am Coll Cardiol* **42:**336–342.

Browner MF, Smith WW, and Castelhano AL (1995) Matrilysin-inhibitor complexes: common themes among metalloproteases. *Biochemistry* **34:**6602–6610.

Crawford HC, Scoggins CR, Washington MK, Matrisian LM, and Leach SD (2002) Matrix metalloproteinase-7 is expressed by pancreatic cancer precursors and regulates acinar-to-ductal metaplasia in exocrine pancreas. *J Clin Investig* **109:** 1437–1444.

Davies G, Jiang WG, and Mason MD (2001) Matrilysin mediates extracellular cleavage of E-cadherin from prostate cancer cells: a key mechanism in hepatocyte growth factor/scatter factor-induced cell-cell dissociation and in vitro invasion. *Clin Cancer Res* **7:**3289–3297.

Egeblad M and Werb Z (2002) New functions for the matrix metalloproteinases in cancer progression. *Nat Rev Cancer* **3:**161–174.

Fu X, Kassim SY, Parks WC, and Heinecke JW (2001) Hypochlorous acid generated by myeloperoxidase modifies adjacent tryptophan and glycine residues in the catalytic domain of matrix metalloproteinase-7: an oxidative mechanism for restraining protease activity during inflammation. *J Biol Chem* **276:**41279–41287.

Hamuro Y, Wong L, Shaffer J, Kim JS, Jennings PA, Adams JA, and Woods VL Jr (2002a) Phosphorylation-driven motion in the COOH-terminal Src kinase, Csk, revealed through enhanced hydrogen-deuterium exchange and mass spectrometry (DXMS). *J Mol Biol* **323:**871–881.

Hamuro Y, Zawadzki KM, Kim JS, Stranz D, Taylor SS, and Woods VL Jr (2003) Dynamics of cAPK type IIb activation revealed by enhanced amide H/2H exchange mass spectrometry (DXMS). *J Mol Biol* **327:**1065–1076.

Hamuro Y, Zawadzki K, Kim JS, Taylor SS, and Woods VL Jr (2002b) Dynamics of protein kinase A regulatory subunit studied by enhanced hydrogen deuterium exchange-mass spectrometry (DXMS). *Protein Sci* **11:**84.

Heppner KJ, Matrisian LM, Jensen RA, and Rodgers WH (1996) Expression of most matrix metalloproteinase family members in breast cancer represents a tumor-induced host response. *Am J Pathol* **149:**273–282.

Khan MA, Muzammil S, and Musarrat J (2002) Differential binding of tetracyclines with serum albumin and induced structural alterations in drug-bound protein. *Int J Biol Macromol* **30:**243–249.

Kisker C, Hinrichs W, Tovar K, Hillen W, and Saenger W (1995) The complex formed between Tet repressor and tetracycline-Mg^{2+} reveals mechanism of antibiotic resistance. *J Mol Biol* **247:**260–280.

Kivela-Rajamaki M, Maisi P, Srinivas R, Tervahartiala T, Teronen O, Husa V, Salo T, and Sorsa T (2003) Levels and molecular forms of MMP-7 (matrilysin-1) and MMP-8 (collagenase-2) in diseased human peri-implant sulcular fluid. *J Periodontal Res* **38:**583–590.

Lakowicz JR (1983) *Principles of Fluorescence Spectroscopy*. Plenum Press, New York.

Lindsey M (2004) MMP induction and inhibition in myocardial infarction. *Heart Fail Rev* **9:**7–19.

Lowry CL, McGeehan G, and LeVine H (1992) Metal ion stabilization of the conformation of a recombinant 19-kDa catalytic fragment of human fibroblast collagenase. *Proteins* **12:**42–48.

Matsuno K, Adachi Y, Yamamoto H, Goto A, Arimura Y, Endo T, Itoh F, and Imai K (2003) The expression of matrix metalloproteinase matrilysin indicates the degree of inflammation in ulcerative colitis. *J Gastroenterol* **38:**348–354.

Miller EJ and Rhodes RK (1982) Preparation and characterization of the different types of collagen. *Methods Enzymol* **82:**33–64.

Nagase H (1997) Activation mechanisms of matrix metalloproteinases. *Biol Chem* **378:**151–160.

Okamoto T, Akaike T, Sawa T, Miyamoto Y, vanderVliet A and Maeda H (2001) Activation of matrix metalloproteinases by peroxynitrite-induced protein *S*-glutathiolation via disulfide S-oxide formation. *J Biol Chem* **276:**29596–29602.

Onoda T, Ono T, Dhar DK, Yamanoi A, Fujii T, and Nagasue N (2004) Doxycycline inhibits cell proliferation and invasive potential: combination therapy with cyclooxygenase-2 inhibitor in human colorectal cancer cells. *J Lab Clin Med* **143:**207–216.

Pantazatos D, Kim JS, Klock HE, Stevens RC, Wilson IA, Lesley SA, and Woods VL Jr (2004) Rapid refinement of crystallographic protein construct definition employing enhanced hydrogen/deuterium exchange mass spectrometry (DXMS). *Proc Natl Acad Sci USA* **101:**751–756.

Peterson JT (2004) Matrix metalloproteinase inhibitor development and the remodeling of drug discovery. *Heart Fail Rev* **9:**63–79.

Ryan ME, Ramamurthy S, and Golub LM (1996) Matrix metalloproteinases and their inhibition in periodontal treatment. *Curr Opin Periodontol* **3:**85–96.

Schneider S (2001) Proton and metal ion binding by tetracyclines, in *Tetracyclines in Biology, Chemistry and Medicine* (Nelson M, Hillen W and Greenwald RA eds) pp 65–104, Birkhauser Verlag, Basel, Switzerland.

Seftor RE, Seftor EA, DeLarco JE, Kleiner DE, Leferson J, Stetler-Stevenson WG, McNamara TF, Golub LM, and Hendrix MJ (1998) Chemically modified tetracyclines inhibit human melanoma cell invasion and metastasis. *Clin Exp Metastasis* **16:**217–225.

Smith GN Jr, Brandt KD, and Hasty KA (1996) Activation of recombinant human neutrophil procollagenase in the presence of doxycycline results in fragmentation of the enzyme and loss of enzyme activity. *Arthritis Rheum* **39**.

Smith GN Jr, Mickler EA, Hasty KA, and Brandt KD (1999) Specificity of inhibition of matrix metalloproteinase activity by doxycycline: relationship to structure of the enzyme. *Arthritis Rheum* **42:**1140–1146.

Suter P and Rosenbusch JP (1977) Determination of the Donnan effect in equilibrium dialysis and a simple method for its correction. *Anal Biochem* **82:**109–114.

Takahashi M, Altschmied L, and Hillen W (1986) Kinetic and equilibrium characterization of the Tet repressor-tetracycline complex by fluorescence measurements. Evidence for divalent metal ion requirement and energy transfer. *J Mol Biol* **187:**341–348.

Thompson RW and Baxter BT (1999) MMP inhibition in abdominal aortic aneurysms. Rationale for a prospective randomized clinical trial. *Ann NY Acad Sci* **878:**159–178.

Villarreal FJ, Griffin M, Omens J, Dillmann W, Nguyen J, and Covell J (2003) Circulation. *108* **12:**1487–1492.

Visse R and Nagase H (2003) Matrix metalloproteinases and tissue inhibitors of metalloproteinases: structure, function and biochemistry. *Circ Res* **92:**827–839.

Wart HEV and Birkedal-Hansen H (1990) The cysteine switch: a principle of regulation of metalloproteinase activity with potential applicability to the entire matrix metalloproteinase gene family. *Proc Natl Acad Sci USA* **87:**5578–5582.

Willenbrock F, Murphy G, Phillips IR, and Brocklehurst K (1995) The second zinc atom in the matrix metalloproteinase catalytic domain is absent in the full-length enzymes: a possible role for the C-terminal domain. *FEBS Lett* **358:**189–192.

Wilson CL, Heppner KJ, Labosky PA, Hogan BL, and Matrisian LM (1997) Intestinal tumorigenesis is suppressed in mice lacking the metalloproteinase matrilysin. *Proc Natl Acad Sci USA* **94:**1402–1407.

Woods VL Jr (2002) High resolution, high throughput amide deuterium exchange-mass spectrometry (DXMS) determination of the dynamics and structure of protein- protein interactions. *J Am Soc Mass Spectrom* **13:**14S.

Woods VL Jr and Hamuro Y (2001) High-resolution, high-throughput amide deuterium exchange-mass spectrometry (DXMS) determination of protein binding site structure and dynamics: utility in pharmaceutical design. *J Cell Biochem* **37:**89–98.

Yamamoto T, Izumi S, and Gekko K (2004) Mass spectrometry on hydrogen/deuterium exchange of dihydrofolate reductase: effects of ligand binding. *J Biochem (Tokyo)* **135:**633–671.

Address correspondence to: Francisco J. Villarreal, Department of Medicine, University of California, San Diego, 9500 Gilman Drive, BSB 0613J, La Jolla, CA 92093. E-mail: fvillarr@ucsd.edu